

# EFFECT OF WATER COLLISION EFFICIENCY ON EMISSIONS OF NON-PREMIXED HYDROGEN/AIR FLAMES

R. Concetti\*, J. Hasslberger\*, M. Klein\*

riccardo.concetti@unibw.de

\*University of the Bundeswehr Munich, Werner-Heisenberg-Weg 39, 85579, Neubiberg,  
Germany

## Abstract

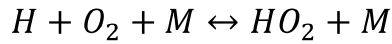
The present study investigates the role of the high collision efficiency of water on the emissions of nitrogen oxides ( $NO_x$ ) in the context of non-premixed flames, which have particular relevance in industrial applications. A series of counterflow hydrogen/air flame simulations has been conducted for a range of water loading levels and strain rates. These simulations employ a state-of-the-art chemical mechanism provided by the CRECK group, and a modified version of the mechanism wherein the third-body reaction efficiency of water is inhibited. The outcomes reveal the potential of mitigating emissions due to the properties of water, particularly under circumstances characterized by elevated strain rates.

## Introduction

The potential of employing steam injection in combustion systems has been explored as a strategy to mitigate greenhouse gas emissions, notably within methodologies like MILD combustion or Exhaust Gas Recirculation. This approach is considered promising for reducing emissions of  $NO_x$  and other deleterious by-products, as documented in the existing literature [1,2]. Nitrogen oxides primarily arise through four pathways:

1. The Zeldovich mechanism or thermal mechanism [3], prevalent under high-temperature conditions.
2. The Prompt or Fenimore mechanism [4], characteristic of rich hydrocarbon combustion.
3. The  $N_2O$  mechanism, observed in environments with elevated concentrations of atomic oxygen.
4. The  $NNH$  mechanism, prominent under conditions with elevated concentrations of atomic hydrogen.

The importance of the high third-body reaction efficiency of water in affecting the flame structure has been analyzed in previous research by Koroll and Mulpuru [5]. They found that when a hydrogen/oxygen premixed flame is diluted with steam at various concentrations, the reduction in flame speed is less than the value predicted by assuming water to be inert. This effect primarily stems from a specific third-body reaction:



This particular reaction's relevance has also been recognized in the studies of Lamioni et al. [6] and Attili et al. [7], where it is characterized as a chain-breaking reaction competing with a non-third-body chain-branching reaction. The balance between these reactions depends on the system temperature and can be influenced by the presence of chemical species that affect the strength of third-body reactions, such as water.

The aim of the current study is to investigate the influence of water injection on a canonical counterflow non-premixed flame, with particular attention to the high third-body reaction efficiency of water. The paper presents the theoretical framework in the next section, then proceeds with the presentation and discussion of results, and concludes by outlining the findings.

### Theoretical Background

The current investigation explores a counterflow non-premixed flame configuration, wherein fuel and oxidizer are injected from opposite directions with predetermined velocities and separation distance. This configuration inherently exhibits a two-dimensional nature and is characterized by a certain degree of strain. The flame structure of such configurations is notably influenced by the level of strain, rendering it a crucial design parameter also analyzed in this study. To consider different strain rate levels, the relationships delineated by Fiala and Sattelmayer [8] are utilized to specify the boundary conditions for fuel and oxidizer. For each adjustment in strain level, the inlet temperature ( $T$ ) and inlet flow composition ( $Y_\alpha$ ) remain constant, while the inlet velocity ( $u$ ) and distance between the two inlets ( $d$ ) are varied according to the subsequent scaling rules:

$$u_{new} = u_{old} \left( \frac{a_{new}}{a_{old}} \right)^{\frac{1}{2}}; d_{new} = d_{old} \left( \frac{a_{new}}{a_{old}} \right)^{-\frac{1}{2}} \quad (1)$$

In this context,  $a$  denotes the strain rate, with the subscript indicating the value corresponding to either the preceding (old) or current simulation (new). This method allows for the utilization of prior simulations, adjusted with the updated distance, as initial solutions, thereby facilitating quicker convergence, as explained by Fiala and Sattelmayer [8]. The software utilized for executing the series of batch simulations is Cantera [9], a widely recognized computational platform for modeling chemical kinetics and transport phenomena. In this investigation, a state-of-the-art mechanism proposed by the CRECK group and considering the chemistry relevant to  $NO_x$  formation, is adopted [10-12]. The mechanism comprises a total of 159 species and 2459 elementary reactions. Employing this established framework, a sequence of analyses is carried out at various levels of strain rate until extinction is reached, with different levels of water loading in the oxidizer inlet mass (i.e.,  $Y_W$  between 0% and

10%). Subsequently, the chemical mechanism is adjusted to isolate the impact of the high third-body reaction efficiency of water, with this parameter set to zero for all elementary reactions.

## Results and Discussion

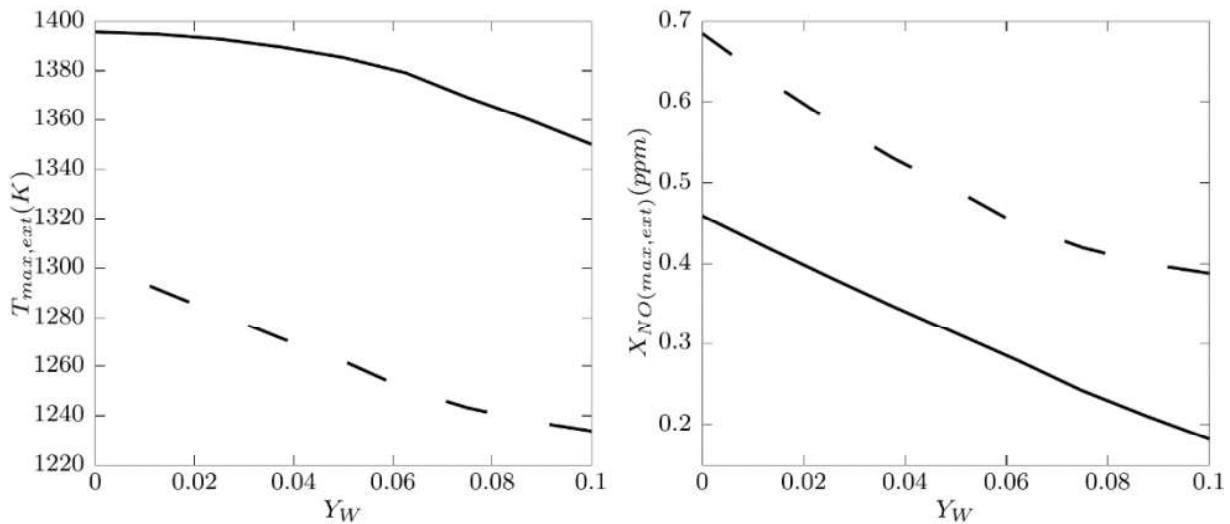


**Figure 1.** Maximum temperature close to the extinction strain rate ( $T_{max,ext}$ ) and maximum nitrogen monoxide molar fraction close to extinction strain rate ( $X_{NO(max,ext)}$ ) for different levels of water loading by mass ( $Y_W$ ). The continuous lines refer to the cases with the original chemical mechanism, while the dashed lines refer to the cases with the mechanism without third-body reaction efficiency of water.

The impact of the high third-body reaction efficiency of water at varying degrees of water loading, under strain rate levels close to quenching, is first considered. As depicted in Fig. 1, which illustrates the maximum temperature and the peak  $NO$  molar fraction for the considered conditions, it becomes clear that both quantities decrease as the water loading increases. However, upon considering the collision efficiency of water, the maximum temperature under extinction conditions exceeds that observed in cases where the collision efficiency is inactive. This supports observations from literature regarding the higher temperatures achieved with water dilution compared to those predicted when steam is considered inert [5]. Additionally, the sign of curvature of the curves representing the temperature trend changes. If only the Zeldovich mechanism is considered, the outcomes from Fig. 1 might seem counterintuitive, given that elevated temperature conditions typically result in increased  $NO$  emissions. However, as written in the introduction, the formation of  $NO_x$  proceeds through different pathways. This leads to the inference that the high third-body reaction efficiency of water profoundly affects radicals production (i.e., H and O), thereby exerting a significant influence on nitrogen oxide emissions. The conditions investigated thus far pertain to scenarios approaching flame extinction. In practical scenarios, various levels of strain rate are encountered

depending on the location within the combustion apparatus. Consequently, our attention now turns to examining the evolution of maximum temperature and maximum nitrogen monoxide emissions at different strain rate levels, with water loading levels of 0%, 5%, and 10%.

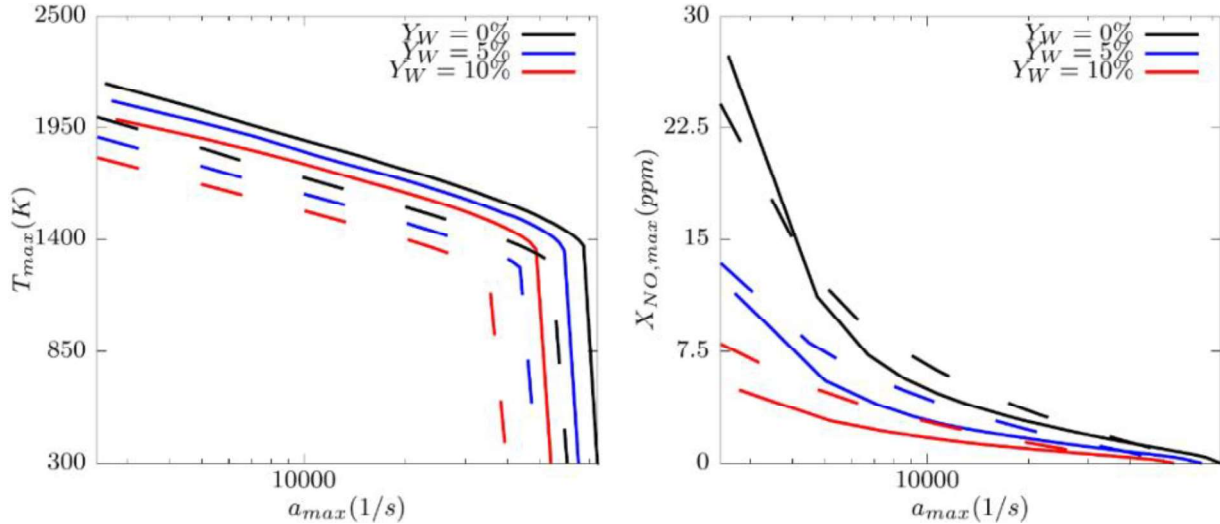


**Figure 2.** Maximum temperature ( $T_{max}$ ) and maximum nitrogen monoxide molar fraction ( $X_{NO,max}$ ) as a function of maximum strain rate ( $a_{max}$ ). The continuous lines refer to the cases with the original chemical mechanism, while the dashed lines refer to the cases with the mechanism without third-body reaction efficiency of water. The different levels of water are indicated in black for 0%, blue for 5% and red for 10%.

Figure 2 illustrates the trends of maximum temperature and nitrogen monoxide molar fraction with strain rate, across the three specified levels of water loading. It becomes evident that the maximum temperature of the systems decreases with increasing strain rate until reaching the quenching level. When the third-body reaction efficiency of water is active, the flame consistently exhibits a higher maximum temperature compared to cases with the modified mechanism. While the temperature demonstrates consistent behavior irrespective of strain rate and water loading, with higher values observed when the collision efficiency is activated, a crossover is observed for the  $NO$  emissions: the emissions of  $NO$  at 0% water loading are higher with the original mechanism and low strain rate levels, subsequently decreasing as conditions approach quenching. With higher steam concentration, the intersection point shifts toward zero strain rate or disappears entirely. This phenomenon may be explained by the varying significance of the system temperature at different strain rate levels. Near zero strain rate, the elevated maximum temperature is assumed to favor the Zeldovich mechanism [3]. However, as the strain rate grows, the system's maximum temperature decreases, leading to increased prominence of other pathways and their strength is correlated with radical concentrations [2].

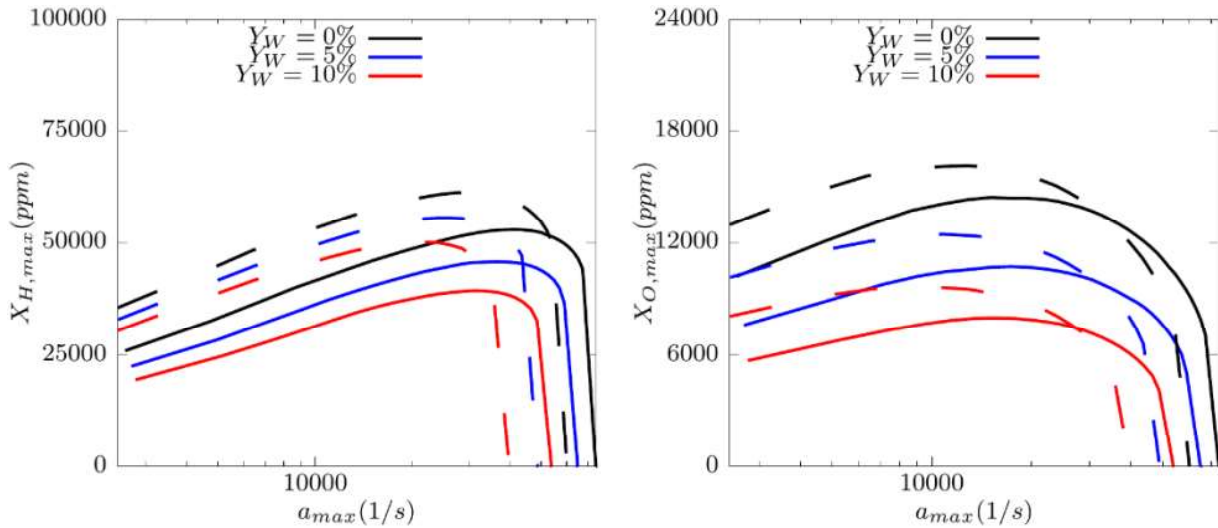


**Figure 3.** Maximum atomic hydrogen molar fraction ( $X_{H,max}$ ) and maximum atomic oxygen molar fraction ( $X_{O,max}$ ) as function of maximum strain rate ( $a_{max}$ ).

The continuous lines refer to the cases with the original chemical mechanism, while the dashed lines refer to the cases with the mechanism without third-body reaction efficiency of water. The different levels of water are indicated in black for 0%, blue for 5% and red for 10%.

From Fig. 3, it is evident that the concentrations of radicals grow with the strain rate for strain rates being sufficiently smaller than the extinction limit, typically being higher with the modified mechanism. This phenomenon explains the elevated emissions of  $NO$  due to the increased importance of the  $NNH$  and  $N_2O$  mechanisms, despite the lower temperature observed (see Fig. 2), for the modified reaction mechanism with third body efficiency set to zero. Nevertheless, the Zeldovich mechanism remains of paramount importance and Fig. 2 suggests a clear correlation between temperature and  $NO$  emissions.

## Conclusion

In this study, a series of Cantera simulations were conducted for non-premixed counterflow hydrogen/air flames. The primary objective was to investigate the impact of water injection on  $NO_x$  emissions, with specific emphasis on the third-body reaction efficiency of water. It was observed that when the collision efficiency of water is active, the flame exhibits higher temperatures at every strain rate level compared to cases employing a modified chemical mechanism. The production of  $NO$  is notably influenced by the collision efficiency; at low strain rates, the original chemical mechanism generates higher pollutant levels when no steam is added, whereas at higher strain rates, the emission of nitrogen monoxide is lower than in cases without collision efficiency. The higher emissions observed with the modified mechanism are attributed to the increased presence of radicals in the flame under moderately high strain rate conditions.

In the next step of this research, we would like to analyze the effect of preheating at conditions typically considered in practical applications.

## Acknowledgement

This research, in the frame of project MORE, is funded by dtec.bw – Digitalization and Technology Research Center of the Bundeswehr, which we gratefully acknowledge. dtec.bw is funded by the European Union – Next Generation EU

## References

- [1] Göke, S., Paschereit, C. O., “Influence of steam dilution on nitrogen oxide formation in premixed methane/hydrogen flames” *J. Propul. Power* 29(1): 249–260, (2013)
- [2] Lellek, S., Sattelmayer, T., “NO<sub>x</sub>-formation and CO-burnout in water-injected, premixed natural gas flames at typical gas turbine combustor residence times”, *J. Eng. Gas Turb. Power* 140: 051504, (2018)
- [3] Zeldovich, Y. B., “The oxidation of nitrogen in combustion and explosions”, *J. Acta. Physicochimica*. 21: 577, (1948)
- [4] Fenimore, C., “Studies of fuel-nitrogen species in rich flame gases” *Proc. Comb. Inst.* 17: 661–670, (1979)
- [5] Koroll, G., Mulpuru, S. “The effect of dilution with steam on the burning velocity and structure of premixed hydrogen flames”, *Proc. Comb. Inst.*: 1811–1819, (1988)
- [6] Lamioni, R., Lapenna, P. E., Berger, L., Kleinheinz, K., Attili, A., Pitsch, H., Creta, F., “Pressure-induced hydrodynamic instability in premixed methane-air slot flames” *Combust. Sci. Techno.* 192(11): 1998–2009, (2020)
- [7] Attili, A., Lamioni, R., Berger, L., Kleinheinz, K., Lapenna, P.E., Pitsch, H., Creta, F., “The effect of pressure on the hydrodynamic stability limit of premixed flames” *Proc. Comb. Inst.* 38(2): 1973–1981, (2021)
- [8] Fiala, T., Sattelmayer, T., “Nonpremixed Counterflow Flames: Scaling Rules for Batch Simulations”, *Journal of Combustion* 2014: 484372, (2014)
- [9] Goodwin, D. G., Moffat, H. K., Spath, R. L., “Cantera: an object-oriented software toolkit for chemical kinetics, thermodynamics, and transport processes”, (2018)
- [10] Ranzi, E., Frassoldati, A., Grana, R., Cuoci, A., Faravelli, T., Kelley, A. P., Law, C. K., “Hierarchical and comparative kinetic modeling of laminar flame speeds of hydrocarbon and oxygenated fuels”, *Prog. Energ. Combust.* 38: 468-501, (2012)
- [11] Ranzi, E., Frassoldati, A., Stagni, A., Pelucchi, M., Cuoci, A., Faravelli, T., “Reduced kinetic schemes of complex reaction systems: fossil and biomass-derived transportation fuels”, *Int. J. Chem. Kinet.* 46: 512-542, (2014)
- [12] Song, Y., Marrodan, L., Vin, N., Herbinet, O., Assaf, E., Fittschen, C., Stagni, A., Faravelli, T., Alzueta, M. U., Battin-Leclerc, F., “The sensitizing effects of NO<sub>2</sub> and NO on methane low temperature oxidation in a jet stirred reactor”, *Proc. Comb. Inst.* 37: 667-675, (2019)